Available online at www.sciencedirect.com

ScienceDirect

Ceramics International 35 (2009) 1377–1383

CERAMICS INTERNATIONAL

www.elsevier.com/locate/ceramint

Hot pressing of bimodal alumina powders with magnesium aluminosilicate (MAS) addition

Jiang Li *, Yubai Pan, Liping Huang, Jingkun Guo

Shanghai Institute of Ceramics, Chinese Academy of Sciences, 1295 Dingxi Road, Shanghai 200050, China

Received 13 May 2008; received in revised form 19 June 2008; accepted 14 July 2008
Available online 5 August 2008

Abstract

High quality alumina ceramics were fabricated by hot-pressed sintering using bimodal alumina with superfine component as raw material and magnesium aluminosilicate (MAS) glass as sintering aid. Densification behavior, microstructure evolution and mechanical properties of alumina were investigated from 1300 °C to 1450 °C. The bimodal alumina powders were sintered to 99.8% of the theoretical value at 1400 °C and a comparative dense microstructure with a few plate-like abnormal grains was observed. With increase of sintering temperature up to 1450 °C, many fine matrix grains were consumed and quite a few abnormal grains impinged upon each other. For the alumina ceramics hot-pressed from bimodal alumina with 30 wt.% superfine component, optimal mechanical properties were obtained at 1400 °C. The bending strength and fracture toughness were 522 MPa and 5.0 MPa $m^{1/2}$, respectively.

Keywords: Bimodal alumina; Hot pressing; Microstructure; Mechanical properties

1. Introduction

Packing and densification characteristics of bimodal alumina powders have been studied in previous works [1,2]. The bimodal alumina powder mixtures increased the density of green compacts, enhanced the densification of low-reactivity coarse powder and improved the microstructure of ceramics. Nevertheless, solid-state sintering of bimodal alumina generally requires high temperatures. In order to lower sintering temperature, oxides or glass-forming systems were introduced to induce liquid-phase sintering [3]. The process of liquid-phase sintering has been classified into three distinct stages [4,5]: (1) particle rearrangement [6], (2) solution-diffusion-precipitation [7] and (3) final pore removal [8]. The small amounts of liquid-forming additives could significantly enhance densification kinetics by liquid-phase sintering. In our previous work, bimodal alumina powders with superfine component were pressureless-sintered using MgO and SiO_2 as additives [9]. The effects of superfine alumina and sintering aids on the densification, microstructure evolution and mechanical properties were investigated. It was found that hot pressing alumina resulted in a synergistic effect on densification and higher density could be obtained than during pressureless-sintering. Particle rearrangement by boundary sliding is suggested as the process responsible for the initial increase in compact density [10]. It is concluded that the final stage of densification of alumina during hot pressing occurs by enhanced diffusion under the influence of stress [11].

Conventional processes for synthesizing α-Al_2O_3 involve mechanical milling [12], vapor phase reaction [13,14], precipitation [15–17], sol–gel [18,19], hydrothermal [20] and combustion methods [21–24]. In the present work, high-purity commercial α-Al_2O_3 and superfine α-Al_2O_3 synthesized by precipitation method were used to prepare bimodal alumina powders, with magnesium aluminosilicate (MAS) glass as sintering aid. Alumina ceramics were prepared by hot pressing at different temperatures. The densification, the microstructure evolution and mechanical properties of alumina ceramics were investigated. For comparison, pressureless-sintering of bimodal alumina was also studied in this paper.

2. Experimental

Superfine α-Al_2O_3 was prepared by a precipitation method with $NH_4Al(SO_4)_2\cdot 12H_2O$ (A.R., Jinshan Chemical Co.,

---

* Corresponding author. Tel.: +81 21 52412816; fax: +81 21 52413903.
E-mail address: lijiang@mail.sic.ac.cn (J. Li).

0272-8842/$34.00 © 2008 Elsevier Ltd and Techna Group S.r.l. All rights reserved.
doi:10.1016/j.ceramint.2008.07.002

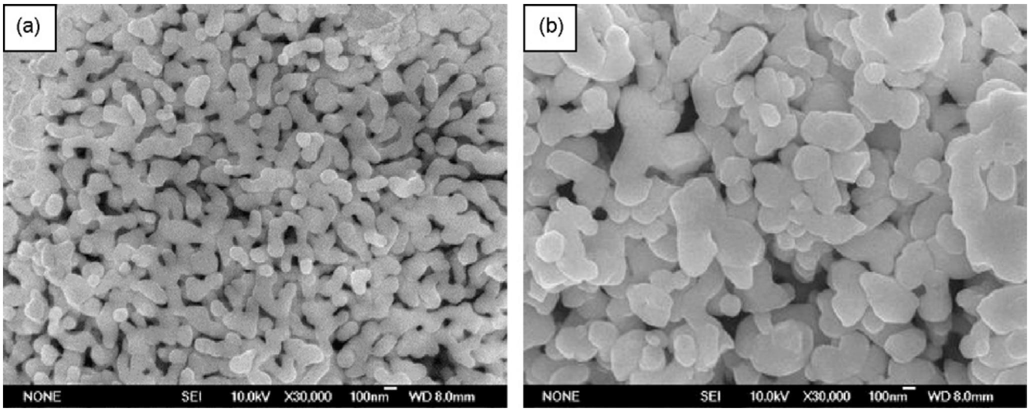

Fig. 1. FESEM micrographs of (a) the synthesized α-Al_2O_3 and (b) the commercial α-Al_2O_3.

Shanghai, China) and NH_4HCO_3 (A.R., Hewei Chemical Co., Shanghai, China) as raw materials. The process for preparing α-Al_2O_3 powders is the same as reported in our previous work [9]. The superfine α-Al_2O_3 powders obtained and commercial coarse-grained-alumina powders (A.R., Wusong Chemical Co., Shanghai, China) with the median particle of about 0.5 μm were used to prepare bimodal alumina mixtures. The weight percents of the prepared superfine α-Al_2O_3 were 0%, 10% and 30%, respectively. One wt.% of ternary eutectic magnesium aluminosilicate (MAS) glass (17.5 MgO, 21.5 Al_2O_3 and 61.0 SiO_2 in wt.%) was added as sintering aid and mixed with bimodal alumina powders. All the powder mixtures were dispersed in ethanol and ball-milled with high-purity alumina balls for 24 h in plastic containers. After drying, the powders were screened through a 200-mesh sieve. The screened powder mixtures were die-pressed in a BN-coated graphite die into a rectangular shape of 30 mm × 35 mm at room temperature. The samples were sintered for 1 h at different temperatures under a pressure of 20 MPa in a nitrogen gas atmosphere with a high-purpose furnace (High-MULTI 10000). For comparison, a portion of screened powder mixtures were uniaxially pressed into bars (6 mm × 8 mm × 45 mm) under a pressure of 100 MPa and then sintered at different temperatures in air with a heating rate of 5 °C min^{-1} and a dwelling time of 3 h at the maximum temperature.

The morphology of the powders was investigated by field emission scanning electron microscopy (FESEM) (Model JSM-6700, JEOL, Tokyo, Japan). The bulk densities of the sintered samples were measured by the Archimedes method. Microstructures of the fractured surfaces were observed with a scanning electron microscopy (SEM) (Model EPMA-8705QH2, Shimadzu, Tokyo, Japan). A transmission electron microscopy (TEM) (Model JEM-2010, JEOL, Tokyo, Japan) equipped with X-ray energy dispersive spectroscopy (EDS) (Model Link ISIS-300, Oxford, England) was used to characterize the morphology and the chemical composition of the alumina ceramics. The sintered samples were machined into bars of 3 mm × 4 mm × 36 mm after being ground and polished. The bending strength and fracture toughness of the sintered samples were measured at room temperature. The three-point bending test was done in a universal testing machine (Model Instron-1195, INSTRON, Canton, USA) with a span of 30 mm between the supports and a cross-head speed of 0.5 mm min^{-1}. The bending strength for each batch was taken as the average of the strength of the six samples. Fracture toughness values (K_{IC}) were determined by crack indentation

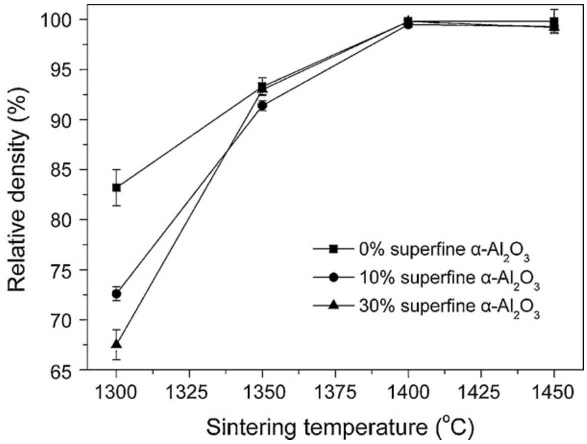

Fig. 2. Relative density of hot-pressed alumina ceramics as a function of sintering temperature.

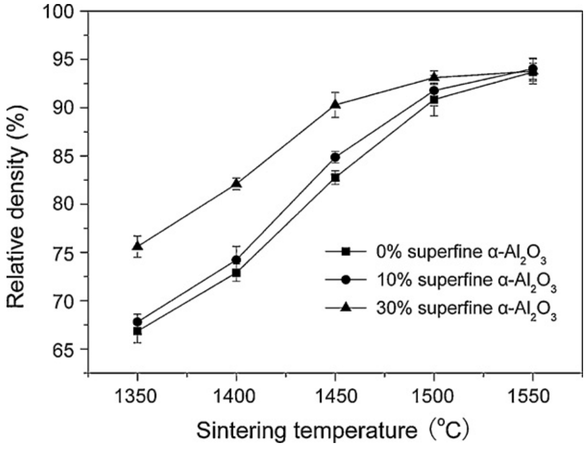

Fig. 3. Relative density of pressureless-sintered alumina ceramics as a function of sintering temperature.

technique in a materials testing machine (Model Instron Wilson-Wolpert-Tukon 2100B, INSTRON, Canton, USA) under load of 49 N, using the equation given by Niihara et al. [25]:

$$K_{IC} = 0.0089\left(\frac{E}{H_V}\right)^{0.4} Pa^{-1} l^{-0.5} \quad \left(0.25 \le \frac{l}{a} \le 2.5\right)$$

where H_V is the Vickers hardness, E is the elastic modulus, P is the indentation load, a is the length of the half-diagonal of the indent, $l = c - a$, and c is the half-length of the indentation crack. The fracture toughness for samples was taken as the average value of six data points.

3. Results and discussion

Fig. 1 shows the micrographs of the synthesized α-Al_2O_3 and of the commercial α-Al_2O_3 powders. It was found that the average particle sizes were ~150 nm and 500 nm, respectively.

Fig. 2 shows a plot of the relative density of hot-pressed alumina ceramics as a function of sintering temperature. It could be seen that the addition of superfine alumina retrained the densification at the temperature of 1300 °C. However, with increase of sintering temperature up to 1350 °C, the effect of superfine alumina on densification became unobvious. At the temperature from 1350 °C to 1400 °C, the increase of temperature distinctly enhanced densification and the relative

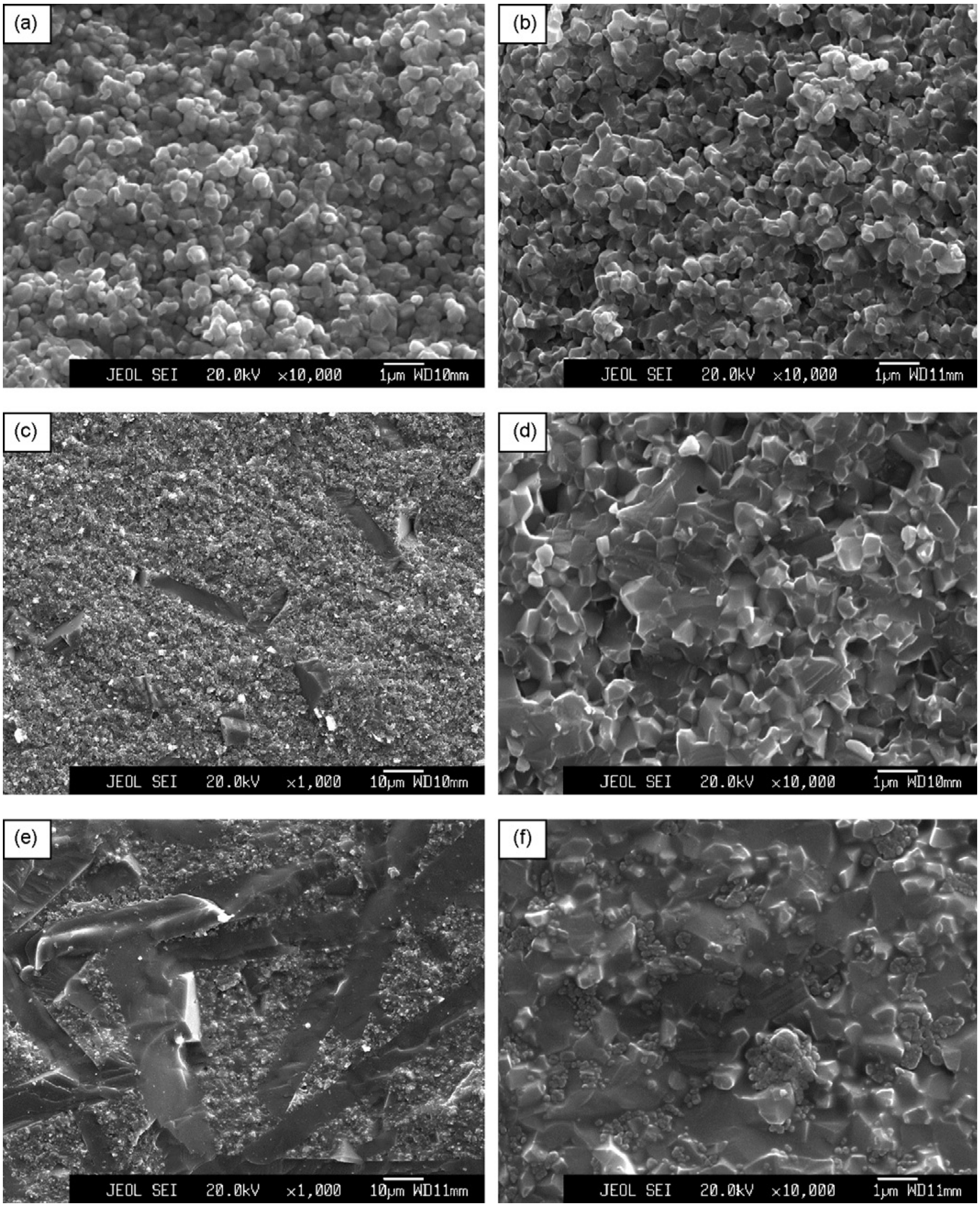

Fig. 4. EPMA micrographs of fracture surfaces of hot-pressed alumina ceramics from commercial alumina with 1.0 wt.% MAS glass sintered at (a) 1300 °C, (b) 1350 °C, (c, d) 1400 °C and (e, f) 1450 °C for 1 h.

densities reached 99.8% of the theoretical value (3.95 g cm^{-3}). With further increase of temperature, the density kept almost unchanged.

Fig. 3 shows the relation between the relative density of pressureless-sintered alumina ceramics and sintering temperature. It was found that the superfine component was effective to enhance the densification at the temperature of 1350–1500 °C and the density rapidly increased with temperature. However, even at the high temperature of 1550 °C, the densities were all lower than 95%. So compared with pressureless sintering, hot pressing bimodal alumina resulted in a synergistic effect on densification and much higher density could be obtained.

Fig. 4 shows the EPMA micrographs of the fracture surfaces of hot-pressed alumina ceramics from commercial alumina with 1.0 wt.% MAS glass sintered at the temperature range of 1300–1450 °C for 1 h. In accordance with the density revealed by the Archimedes method, significant elimination of pores occurred (Fig. 4a and b), and a comparative dense microstructure with a few plate-like abnormal grains was observed at the temperature of 1400 °C. Two magnifications in Fig. 4c and d were used to show both micrographs of the general and the local areas. The microstructure of the specimen sintered at 1450 °C showed typical abnormal grain growth (AGG) and the structure with equiaxed small grains located in skeleton of large elongated grains, as shown in Fig. 4e and f.

Fig. 5 shows the EPMA micrographs of the fracture surfaces of hot-pressed alumina ceramics from bimodal alumina with 30 wt.% superfine component sintered at 1300–1450 °C for 1 h.

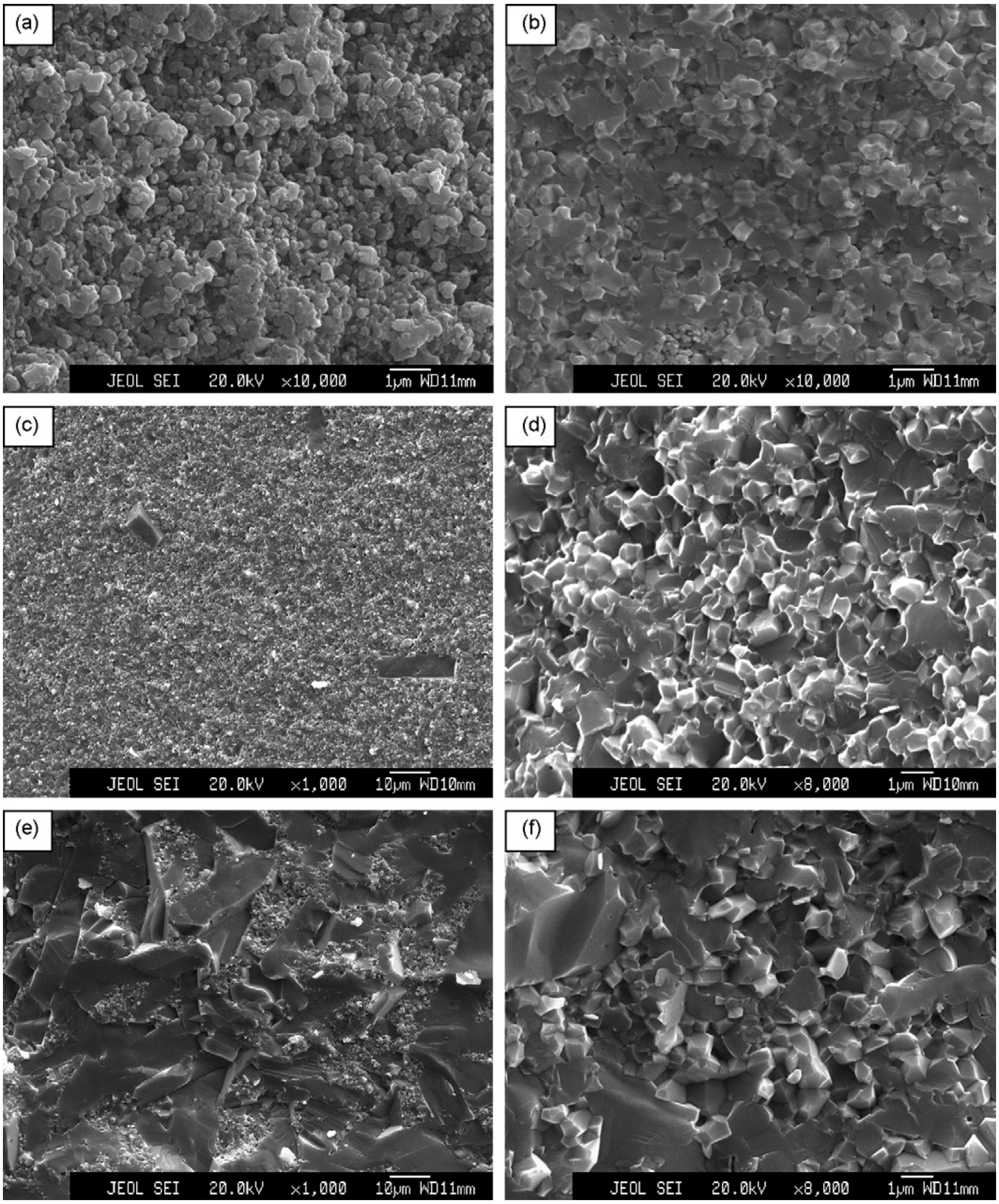

Fig. 5. EPMA micrographs of fracture surfaces of hot-pressed alumina ceramics from bimodal alumina (30 wt.% superfine component) with 1.0 wt.% MAS glass sintered at (a) 1300 °C, (b) 1350 °C, (c, d) 1400 °C and (e, f) 1450 °C for 1 h.

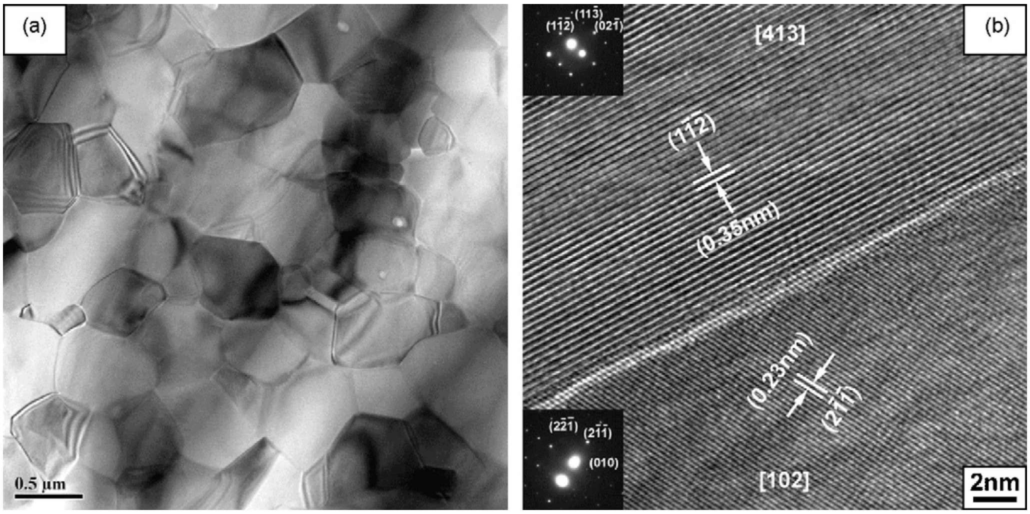

Fig. 6. (a) TEM micrograph of hot-pressed alumina ceramic from bimodal alumina with 30 wt.% superfine component sintered at 1400 °C for 1 h and (b) the HRTEM image of the grain boundary of the hot-pressed alumina ceramic from bimodal alumina with 30 wt.% superfine component sintered at 1400 °C for 1 h.

The grain size increased and pores were gradually removed with increase of sintering temperature. For the specimen sintered at 1350 °C, the microstructure was homogeneous with equiaxed grain size of ~0.5 μm on average, as shown in Fig. 5b. At 1400 °C, the formed MAS liquid phase resulted in pronounced anisotropic and abnormal grain growth. In Fig. 5c, a few abnormal grains, ~15-μm long and ~5-μm wide, have developed and are dispersed in a matrix composed of ~1-μm equiaxed grains. The flat boundary of the abnormal grain is known to be the {0 0 0 1} basal plane [26]. The appearance of the flat boundaries might indicate the presence of continuous liquid films [27]. With further increase of sintering temperature up to 1450 °C, many fine matrix grains were consumed and quite a few abnormal grains had impinged upon each other, as shown in Fig. 5d. It has been well-established that MgO-doping prevents abnormal grain growth during solid-state sintering of alumina [28,29]. Abnormal grain growth is induced by the inhomogeneous distribution of cations in pure alumina [30]. MgO was reported to minimize the effect of chemical inhomogenity by increasing the bulk solubility and reducing or eliminating the liquid phase [31]. In our work, MAS liquid phase formed at the temperature higher than 1365 °C (the eutectic temperature) and AGG in alumina is critically affected by the amount of liquid forming impurities. The higher the liquid content, the larger number of abnormal grains grows abnormally. As a result, a typical bimodal microstructure of AGG with large grains impinged upon each other in equiaxed fine grains because the liquid phase formed was very limited.

Fig. 6a shows the TEM micrograph of alumina ceramic from bimodal alumina with 30 wt.% superfine component sintered at 1400 °C for 1 h. It could be seen that the grains were equiaxed and the average grain size was about 0.5 μm. A high-resolution TEM (HRTEM) micrograph of the grain boundary is displayed in Fig. 6b. The grain boundaries were clean and no amorphous phase was detected at the grain boundaries between equiaxed grains. The interplanar spacing of the top left grain is about 0.35 nm, which corresponds to the distance between two $(1\,\bar{1}\,\bar{2})$ planes of rhombohedral alumina. The interplanar spacing of the right bottom grain is about 0.23 nm, which corresponds to the distance between two $(2\,\bar{1}\,\bar{1})$ planes of rhombohedral alumina. The insets in Fig. 6b are the corresponding SAED patterns of both alumina grains. Because of small quantity of MAS glass added, liquid phase was not detected at the grain boundaries. Spinel might be formed by chemical reaction between MAS glass and alumina and both magnesium consumption by spinel crystallization and alumina dissolution led to mullite nucleation [32,33]. For the alumina ceramics pressureless-sintered at 1550 °C for 3 h from commercial alumina and bimodal alumina with 30 wt.% superfine component, there were many pores in both samples, as shown in Fig. 7.

Fig. 8 shows the bending strength of hot-pressed alumina ceramics as a function of sintering temperature. The increase of temperature considerably enhanced the bending strength of alumina ceramics at a temperature range of 1300–1400 °C mainly because of the enhancement of the density. The drastic degradation of bending strength with increasing temperature up to 1450 °C was attributed to the abnormal grain growth of alumina. At 1300 °C, the bending strength of alumina ceramics decreases with increase of the content of superfine component, due to the decrease of bulk density. For the 1350 °C-, 1400 °C- and 1450 °C-sintered alumina ceramics, the higher content of superfine component was, the higher bending strength obtained. The higher bending strength was due to the presence of more uniform, equiaxed, and fine grains in the microstructure. The maximum bending strength of 1400 °C-sintered alumina ceramics from bimodal alumina with 30 wt.% superfine component was 522 MPa.

The fracture toughness for the hot-pressed alumina ceramics is given as a function of the sintering temperature in Fig. 9. There was a distinct enhancement in fracture toughness at the temperature from 1300 °C to 1400 °C because of the densification of alumina ceramics. For the 1400 °C-hot-pressed alumina ceramics, the high fracture toughness of about 5.0 MPa $m^{1/2}$ was afforded by the relatively uniform, equiaxed and fine-grain microstructure whose fracture mode was almost intergranular. With increase of sintering temperature up to

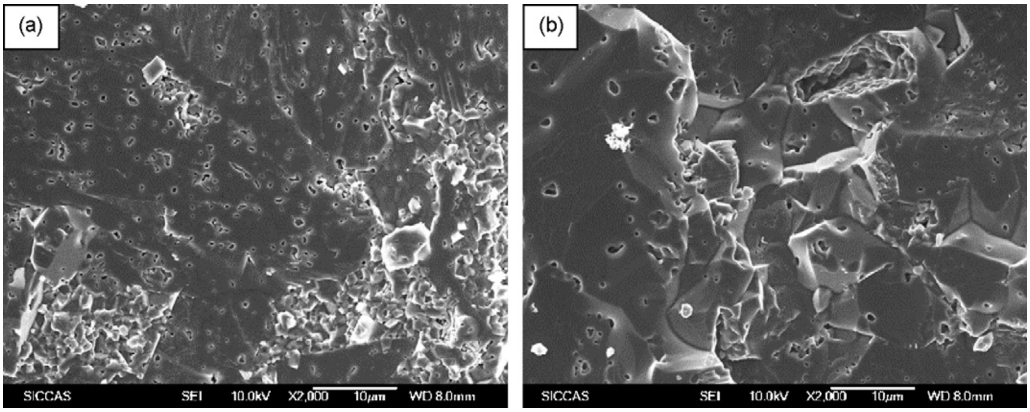

Fig. 7. EPMA micrographs of fracture surfaces of pressureless-sintered alumina ceramics from (a) commercial alumina, (b) bimodal alumina with 30 wt.% superfine component sintered at 1550 °C for 3 h.

1450 °C, there was a decrease due to the increase of the transgranular surface. Relative to intergranular fracture, transgranular fracture in the alumina probably reduces the crack deflection and decreases the critical strain energy release rate. For the samples hot-pressed at 1300 °C and 1350 °C, fracture toughness decreased with increase of the content of superfine component due to the decrease of density. The fracture toughness date of the 1400 °C hot-pressed alumina ceramics from bimodal alumina with different content of superfine component were almost identical, as was due to the similar density and microstructure. At 1450 °C, fracture toughness increased with increase of superfine α-Al_2O_3 due to more equiaxed and fine grains inside the skeleton of abnormal grown grains.

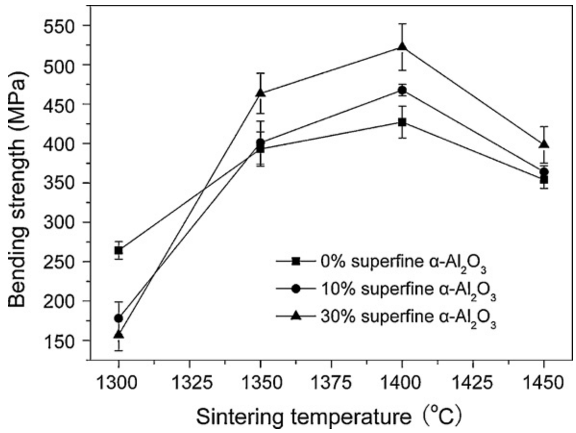

Fig. 8. Bending strength of hot-pressed alumina ceramics from bimodal alumina with 30 wt.% superfine component as a function of sintering temperature.

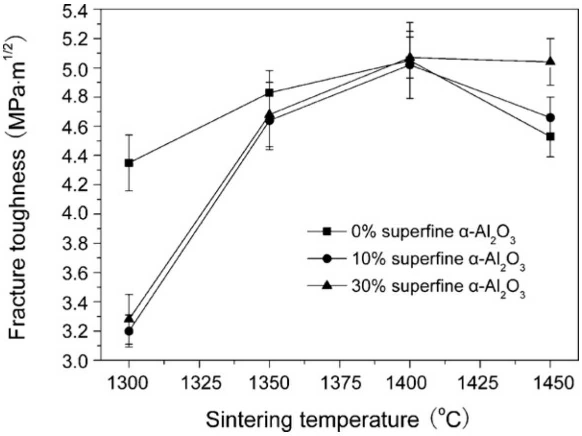

Fig. 9. Fracture toughness of hot-pressed alumina ceramics from bimodal alumina with 30 wt.% superfine component as a function of sintering temperature.

4. Conclusions

High quality alumina ceramics were fabricated by hot pressing using bimodal alumina as raw material and magnesium aluminosilicate (MAS) glass as sintering aid. The bimodal alumina with 30 wt.% superfine component was sintered to 99.8% of the theoretical value at 1400 °C and a few plate-like abnormal grains were observed in the matrix of fine, equiaxied grains. However, with increase of sintering temperature up to 1450 °C, many fine matrix grains were consumed and quite a few abnormal grains impinged. The optimal mechanical properties of the hot-pressed alumina ceramics were obtained at 1400 °C. The bending strength and fracture toughness were 522 MPa and 5.0 MPa $m^{1/2}$, respectively.

Acknowledgements

This work was supported by the Major State Basic Research Development Program of China (973 Program, Grant No. G2000067204-2) the Key Project of Science and Technology of Shanghai (Grant No. 07DJ14001) and the National High-Tech Research and Development Plan (863 Project, Grant No. 2007AA03Z523).

References

[1] J.P. Smith, G.L. Messing, Sintering of bimodally distributed alumina powders, J. Am. Ceram. Soc. 67 (4) (1984) 238–242.

[2] B.G. Ravi, R. Chaim, A. Gedanken, Sintering of bimodal alumina powder mixtures with a nanocrystalline component, Nanostruct. Mater. 11 (7) (1999) 853–859.

[3] S. Taruta, T. Takano, N. Takusagawa, K. Okada, N. Ôtsuka, Liquid phase sintering of bimodal size distributed alumina powder mixtures, J. Mater. Sci. 31 (3) (1996) 573–579.

[4] W.D. Kingery, Densification during sintering in the presence of a liquid phase. I. Theory, J. Appl. Phys. 30 (3) (1958) 301–306.

[5] W.M. Dong, H. Jain, M.P. Harmer, Liquid phase sintering of alumina. I. Microstructure evolution and densification, J. Am. Ceram. Soc. 88 (7) (2005) 1702–1707.

[6] W.J. Huppmann, H. Riegger, Modelling of rearrangement process in liquid phase sintering, Acta Metall. 23 (1975) 965–971.

[7] O.H. Kwon, G.L. Messing, Kinetic analysis of solution-precipitation during liquid phase sintering of alumina, J. Am. Ceram. Soc. 73 (2) (1990) 275–281.

[8] W.M. Dong, H. Jain, M.P. Harmer, Liquid phase sintering of alumina. III. Effect of trapped gases in pores on densification, J. Am. Ceram. Soc. 88 (7) (2005) 1714–1719.

[9] J. Li, Y.B. Pan, F.Q. Qiu, L.P. Huang, J.K. Guo, Alumina ceramics fabricated from bimodal alumina powder mixtures with additives, Mater. Sci. Eng. A 435–436 (2006) 611–619.

[10] E.J. Felten, Hot-pressing of alumina powders at low temperatures, J. Am. Ceram. Soc. 44 (8) (1961) 381–385.

[11] R.L. Coble, J.S. Ellis, Hot-pressing alumina mechanisms of material transport, J. Am. Ceram. Soc. 46 (9) (1965) 438–441.

[12] M.L. Panchula, J.Y. Ying, Mechanical synthesis of nanocrystalline α-Al_2O_3 seeds for enhanced transformation kinetics, Nanostruct. Mater. 9 (1–8) (1997) 161–164.

[13] K. Kamata, T. Mochizuki, S. Matsumoto, A. Yamada, K. Miyokawa, Preparation of submicrometer Al_2O_3 powder by gas-phase oxidation of tris(acetylacetonato) alumina (III), J. Am. Ceram. Soc. 68 (8) (1985), C-193–C-194.

[14] H.K. Varma, T.V. Mani, A.D. Damodran, Characteristics of alumina powders prepared by spray-drying of boehmite sol, J. Am. Ceram. Soc. 77 (6) (1994) 1597–1600.

[15] J.G. Li, X.D. Sun, Synthesis and sintering behavior of a nanocrystalline α-alumina powder, Acta Mater. 48 (12) (2000) 3103–3112.

[16] J. Li, Y.B. Pan, J.W. Ning, L.P. Huang, J.K. Guo, The effect of α-Al_2O_3 seeds on the phase transformation and microstructure of alumina, J. Inorg. Mater. 19 (6) (2004) 1293–1297.

[17] J. Li, Y.S. Wu, Y.B. Pan, J.K. Guo, Influence of fluorides on phase transition of α-Al_2O_3 formation, Ceram. Int. 33 (6) (2007) 919–923.

[18] E. Ponthieu, E. Payen, J. Grimblot, Ultrafine alumina powders via sol–emulsion–gel method, J. Non-Cryst. Solids 147–148 (1992) 598–605.

[19] W.M. Zeng, L. Gao, J.K. Guo, A new sol–gel route using inorganic salt for synthesizing Al_2O_3 nanopowders, Nanostruct. Mater. 10 (4) (1998) 543–550.

[20] A.J. Fanelli, J.V. Burlew, Preparation of fine alumina powder in alcohol, J. Am. Ceram. Soc. 69 (8) (1986), C-174–C-175.

[21] J. Li, Y.B. Pan, C.S. Xiang, Q.M. Ge, J.K. Guo, Low temperature synthesis of ultrafine α-Al_2O_3 powder by a simple aqueous sol–gel process, Ceram. Int. 32 (5) (2006) 587–591.

[22] J. Li, Y.S. Wu, Y.B. Pan, J.K. Guo, Alumina precursors produced by gel combustion, Ceram. Int. 33 (3) (2007) 361–363.

[23] J. Li, Y.S. Wu, Y.B. Pan, J.K. Guo, Influence of citrate to nitrate ratio on the thermal behavior and chemical environment of alumina gel, Ceram. Int. 33 (5) (2007) 735–738.

[24] J. Li, Y.S. Wu, Y.B. Pan, W.B. Liu, Y. Zhu, J.K. Guo, Agglomeration of α-Al_2O_3 powders prepared by gel combustion, Ceram. Int. 34 (6) (2008) 1539–1542.

[25] K. Niihara, R. Morena, D.P.H. Hasselman, Evaluation of K_{IC} of brittle solid by the indentation method with low crack-to-indent ratios, J. Mater. Sci. Lett. 1 (1) (1982) 13–16.

[26] C.A. Bateman, S.J. Bennison, M.P. Harmer, Mechanisms for the role of magnesia in the sintering of alumina-containing small amounts of liquid phase, J. Am. Ceram. Soc. 72 (7) (1989) 1241–1244.

[27] S.H. Hong, D.Y. Kim, Effect of liquid content on the abnormal grain growth of alumina, J. Am. Ceram. Soc. 84 (7) (2001) 1597–1600.

[28] H. Song, R.L. Coble, Origin and growth kinetics of plate-like abnormal grains in liquid-phase-sintered alumina, J. Am. Ceram. Soc. 73 (7) (1990) 2077–2085.

[29] H. Song, R.L. Coble, Morphology of plate-like abnormal grains in liquid-phase-sintered alumina, J. Am. Ceram. Soc. 73 (7) (1990) 2086–2090.

[30] C.A. Handwerker, P.A. Morris, R.L. Coble, Effects of chemical inhomogeneities on grain growth and microstructure in Al_2O_3, J. Am. Ceram. Soc. 72 (1) (1989) 130–136.

[31] A.P. Goswami, S. Roy, M.K. Mitra, G.C. Das, Impurity-dependent morphology and grain growth in liquid-phase-sintered alumina, J. Am. Ceram. Soc. 84 (7) (2001) 1620–1626.

[32] J. Li, Y.B. Pan, Y.S. Wu, H.M. Kou, J.K. Guo, Microstructure and mechanical properties of hot-pressed *a*-Al_2O_3-seeded γ-alumina ceramics, Int. J. Appl. Ceram. Technol. 4 (3) (2007) 276–284.

[33] A. Nakajima, G.L. Messing, Liquid-phase sintering of alumina coated with magnesium aluminosilicate glass, J. Am. Ceram. Soc. 81 (5) (1998) 1163–1172.